scientific reports

Check for updates

OPEN

Production characteristics and adsorption control mechanism of CO_2-rich CBG wells

Zeyuan Sun[1], Xiaodong Zhang[1,2]✉, Caifang Wu[3,4], Shibing Li[5], Jifu Zhang[5], Xianzhong Li[1] & Shuo Zhang[1]✉

To investigate the productivity laws of coalbed gas (CBG) wells in carbon dioxide (CO_2)-rich coalfield, the Haishiwan coal mine in Yaojie coalfield, Gansu Province, China, which is rich in CO_2 of different concentrations in CBG, was selected as the study area. Using numerical simulation technology, the production capacity of CBG wells was simulated, and the thermodynamic factors influencing gas adsorption differences on production capacity were discussed. Numerical simulation indicates that with the increase of CO_2 concentration, the gas breakthrough time is prolonged, and the gas production first increases and then decreases. Research considers that changes in CBG production capacity result from the combined effects of temperature and pressure on gas adsorption. At shallow coal seams, pressure is the dominant factor that promotes gas adsorption, resulting in increased gas content and production. However, due to the competitive adsorption of CO_2 and methane (CH_4), CO_2 preferentially adsorbs on coal, hindering desorption. Therefore, gas breakthrough in CBG wells with high CO_2 concentration is slower, but the production period is longer. On the contrary, high temperatures inhibit gas adsorption in deeper coal seams, reducing gas content and promoting CH_4 desorption. Therefore, CBG wells with low CO_2 concentration have faster gas breakthroughs, but overall production is lower. The findings of this study help to better understand the drainage characteristics of CO_2-rich CBG wells and provide guidance for developing such resources.

Keywords CO_2-rich coalfield, CBG, Capacity simulation, Adsorption heat

In recent years, the consumption of fossil fuels has been increasing. At the same time, a large amount of greenhouse gas—carbon dioxide (CO_2) has been emitted into the atmosphere, leading to climate warming. CO_2 capture and geological sequestration have been to proposed to alleviate the greenhouse effect caused by CO_2 emissions. Among them, CO_2-enhanced coalbed methane recovery (CO_2-ECBM) has great application prospects[1].

Previous studies show that the geological factors, including the buried depth of coal seam, gas properties, tectonics, etc., have a great influence on the production capacity of coalbed methane (CBM)/coalbed gas (CBG) wells[2–4]. Generally, gas content increases as buried depth increases, resulting in an increase in CBG production[5,6]. However, in deep coal seams, different changes in CBG production may occur beyond the critical depth[7]. The proportion of gas components in the formation has a relatively small impact on shale gas productivity, and the higher the adsorbed gas content in the formation, the longer the production period[8]. In addition, the production capacity of CBM/CBG wells is poor in areas with developed faults and synclinal axes. Conversely, in areas characterized by simpler geological structures, such as stable structural zones and synclinal wings, the production capacity is higher, and the stable production period is longer[9,10]. Vikram et al. focused on the CO_2-enhanced CBG production for a block within the Jharia coalfield of eastern India by numerical simulation[11]. Mu et al. found that the increase of CO_2 injection temperature and pressure would promote CO_2 sequestration and enhance methane (CH_4) recovery[12], however Hou et al. discovered that with the increase of injection temperature, CO_2 reserves and CH_4 production would decrease[13]. Zhou discovered that coal shrinkage and skin factor have a significant role in the CBG production of horizontal wells[14]. Hu et al. considered that increasing

[1]School of Energy Science and Engineering, Henan Polytechnic University, Jiaozuo 454003, Henan, China. [2]Collaborative Innovation Center of Coal-bed Methane and Shale Gas for Central Plains Economic Region Henan Province, Jiaozuo 454003, Henan, China. [3]School of Mineral Resources and Geosciences, China University of Mining and Technology, Xuzhou 221008, Jiangsu, China. [4]Key Laboratory of Coalbed Methane Resource and Reservoir Formation Process, Ministry of Education, Xuzhou 221008, Jiangsu, China. [5]Yaojie Coal Power Group Co., Ltd, Lanzhou 730080, Gansu, China. ✉email: z_wenfeng@163.com; zhangshuo_9112@163.com

the drainage rate can increase the gas production of CBM wells[15]. Huang et al. conducted numerical simulation studies on three well types for the development of shale gas reservoirs with large reservoir thickness and multiple layers, and compared the simulation results with actual production data to verify the reliability of the numerical simulation[16]. Zhang et al. optimized the traditional shale gas production capacity prediction method, established an effective prediction model, and applied the model to a gas reservoir in Southwest China[17].

Due to the different affinities of various gases for coal, competitive adsorption occurs, resulting in differences in gas content and composition within coal seams, which further affects the CBG production capacity. In recent years, the theory of multi-component gas adsorption has yielded rich research results. Cui et al. simulated the adsorption rates of CO_2, CH_4, and nitrogen (N_2) on the same coal by establishing a model, and the results showed that the adsorbate molecule size and pore structure of the coal play an important role in selective gas adsorption and diffusion[18]. Busch et al. studied the binary gas adsorption experiments of CH_4 and CO_2, CH_4 and N_2 respectively, and the results showed that CO_2 was the most advantageous in the competitive adsorption, while CH_4 was more advantageous than N_2[19]. Harphlani et al. showed that coals exhibit higher affinity to CO_2 as compared to methane and the preferential adsorption ratio was between 2:1 and 4:1[20]. Zhou et al. discovered that coal has a stronger adsorption force for CO_2 compared to CH_4, and multi-molecule layer adsorption happens during the adsorption of CO_2 on coal matrix[21]. Asif et al. found that CO_2 was adsorbed at faster rate, and that competitive adsorption of CO_2/CH_4 enhanced the displacement of CH_4 when the CO_2 mole fraction was less than 30%[22]. Therefore, it is of great significance to clarify the adsorption mechanism of coal in order to study the capacity of CBG wells.

In summary, there have been many achievements in research on the CBM/CBG production capacity. However, there are some problems. Firstly, most coal seams are rich in CH_4, and the current ground development practices of CBM/CBG mainly focuses on CH_4. There is little research on the production capacity of CBM/CBG wells affected by different gas components in coal seams. Furthermore, during the process of coal mining, the higher the CO_2 concentration in the coal seam, the greater the probability of outburst accidents occurring[23]. For example, in Metropolitan colliery in Australia, approximately 200 tons of coal and 11,500 m^3 of CO_2 were released during the greatest known outburst[24]. The Yaojie coalfield in Gansu Province, China, is a typical CO_2-rich coalfield, with CO_2 concentration of 10–95% in mine gas, coal and CO_2 outburst accidents have occurred several times in the coalfield since 1977. Therefore, in this study, we collected data from the No.2 coal seam of the Haishiwan coal mine in Yaojie coalfield, and summarized the characteristics of CBG in the study area. On the basis of geological data and drainage data, the characteristics of gas production in CBG wells were illustrated. Then, the production capacity of CO_2-rich CBG wells was simulated through GEM software and the differences in production capacity were discussed. Finally, we revealed the thermodynamic mechanism of the impact of gas adsorption differences on production capacity, which is important for the exploitation of CBG in CO_2-rich coalfields.

Geological setting

Geological structure characteristics

The Haishiwan coal mine, located in the south of Yaojie coalfield on the western margin of Minhe Basin, covers a total area of approximately 28.6 km[23]. Structurally, the Haishiwan coal mine is divided into the secondary structural unit of Minhe Basin. The area experienced the Indochin-Yanshan-Himalayan tectonic movements, resulting in well-developed faults and fold structures. The F_{19} fault is the most prominent and developed fault. The basin stratum is Mesozoic-Cenozoic sedimentary, which generally lacks Paleozoic and Mesozoic sedimentary Triassic deposits, and the basement is Proterozoic metamorphic sedimentary[25]. The Haishiwan coal mine lies roughly in a NNW direction with the F_{19} fault located east of it. Due to the influence of tectonic changes in the basement of the coalfield, the Jurassic strata formed an asymmetric oblique fold with a high north and low south pattern, which together with the F_{19} fault, forms the main tectonic framework of the coal-bearing basin (Fig. 1).

Coal-bearing strata

The coal-bearing strata in Haishiwan coal mine is the second group formation of Yaojie Group, which belongs to Mesozoic Middle Jurassic (Fig. 2). Two of the three coal seams are suitable for mining, namely No.1 coal seam and No.2 coal seam. The No.2 coal seam is the main mining, which is a gently inclined coal seam and dip angle changes from 5° to 15°. No.2 coal seam grows most broadly and steadily, with a thickness ranging from 0 to 59.28 m, a buried depth of 506.72 m to 1,013.14 m, and a gradual deepening from north to south. Coal with an average $R_{o,\,max}$ value of 1.02% is either a non-caking coal or weakly caking coal, exhibiting a medium degree of metamorphosis.

Genesis and formation of CO_2

According to the literature[26,27], the measured $\delta^{13}C_{CO2}$ values range from +1.12‰ to -20.00‰, and most of them are heavier than 8‰ (Fig. 3). The higher the CO_2 concentration, the heavier the $\delta^{13}C_{CO2}$. Meanwhile, most of the CO_2 component accounts for more than 60% of the mine gas, indicating that the CO_2 in the Yaojie coalfield is of inorganic origin[28]. Previous studies have shown that $^3He/^4He$ values range from $(0.6 \pm 0.6)\times10^{-8}$ to $(25.9 \pm 0.3)\times10^{-8}$, and R/Ra values range from 0.0042 to 0.185 (where Ra is the atmospheric value of $^3He/^4He$ and R is the sample value of $^3He/^4He$)[26,27]. These indicate that He is derived from the crust and imply that CO_2 in the Yaojie coalfield is of crustal origin. During the late Jurassic to the early Cretaceous, dynamic-thermal metamorphism of the F_{19} fault led to significant decarbonization of carbonate rocks in the bottom layer of the No.2 coal seam during hydrothermal activity. This decarbonization is the inorganic source of CO_2 in the Yaojie coalfield. The regional geological evolution and multi-periodic movements of the F_{19} fault control the formation, migration, and accumulation of CO_2, ultimately resulting in the high CO_2 contents observed in the Yaojie coalfield[27].

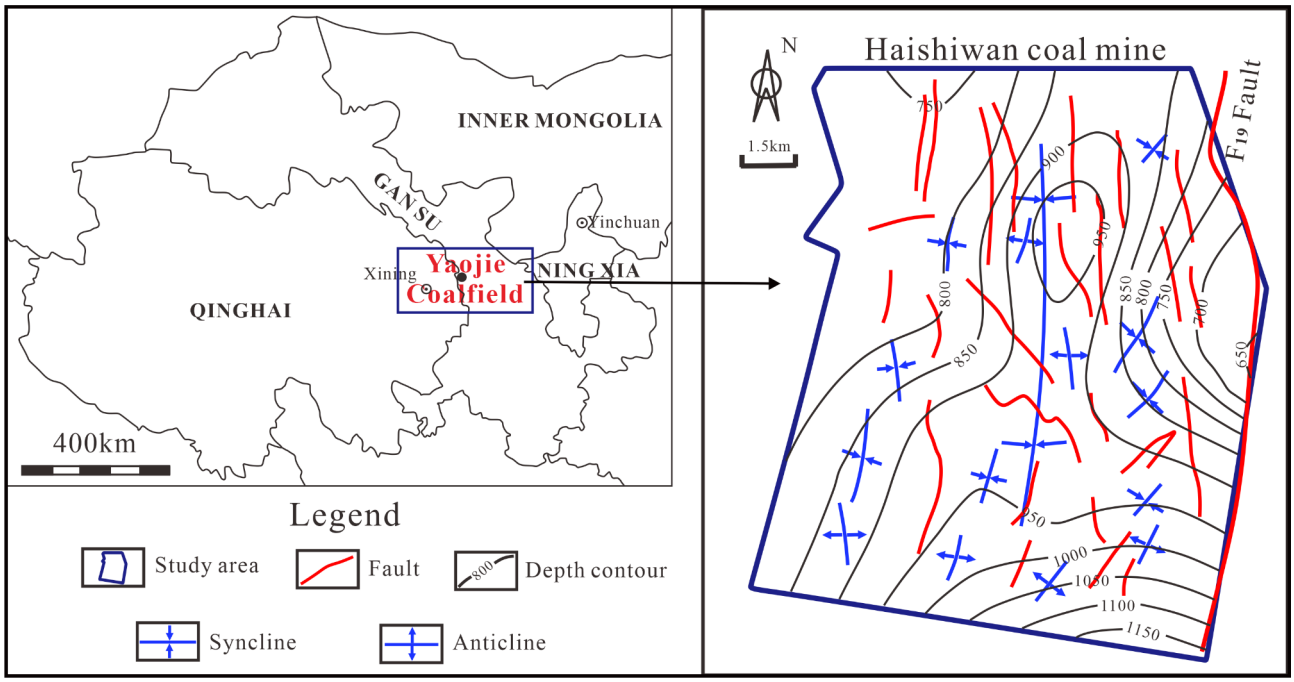

Fig. 1. Location and structure setting of the study area (this figure is generated in CorelDRAW 2020 software, https://www.coreldrawchina.com/).

Engineering overview

The Haishiwan coal mine have started the drilling work of CBG wells from 2019, and 30 CBG wells have been built so far. The well type has evolved from vertical wells to directional and L-shaped horizontal wells. According to the geological background, gas composition and characteristics of gas production, four vertical wells (D2#, D5#, D6#, D8#) were selected as the study objects and the engineering overview of these wells is shown in Table 1. Well D2# is located in the east part of the coal mine, close to the mining face in the west and the F_{19} fault in the east. Wells D5#, D6#, and D8# are situated in the south part of the coal mine and far from the F_{19} fault.

Samples and methods

Gas content test

Coal samples were collected through the rope coring method from CBG wells in the Haishiwan coal mine. First, the desorption gas from coal samples was measured and collected by the canister desorption method employing a standard desorption device in the field test in accordance with the national standard GB/T 19,559 – 2008. It should be emphasized that the gas content on the basis of air-drying is determined by the sum of the natural desorption gas content, escaped gas content and residual gas content. And the escaped gas content was measured using the direct method of the United States Bureau of Mines (USBM)[29,30]. In this paper, the gas content is expressed on the basis of air-drying.

Gas composition analysis

20 groups of gas samples were collected from 20 boreholes in the Haishiwan coal mine. These samples were collected using the drainage gas collection method and stored in water-sealed glass bottles. Each gas sample was collected about 200–400 mL for gas composition analysis. Gas composition was performed using a GC9720Plus gas chromatograph manufactured by Foley Analytical Instruments in accordance with the national standard GB/T 13,610 – 2020 "Gas Chromatography for Compositional Analysis of Natural Gas".

Numerical simulation method

GEM software is capable of simulating dual-porosity dual-permeability reservoirs, including gas adsorption, gas diffusion, and two-phase flow through the natural fracture system[31]. The coal seam is a dual-porosity medium, and the nonlinear desorption of CH_4 in the coal matrix varies over time, described by isotherms related to the gas content and pressure of the matrix. Therefore, to investigate the impact of CO_2 concentration on CBG production, this study employs GEM for numerical simulation. By constructing a model that aligns with the geological background of the study area's CBG development, the study explores the production characteristics. Simulation of multi-component adsorption uses the extended Langmuir isotherm. In this study, No.2 coal seam was selected as an example for simulation reaseach. The model was 30 × 30 blocks each with a length of 10 m. The model doesn't take into account the inclusion of gangue in the coal seams. Table 2 reveals the Model description.

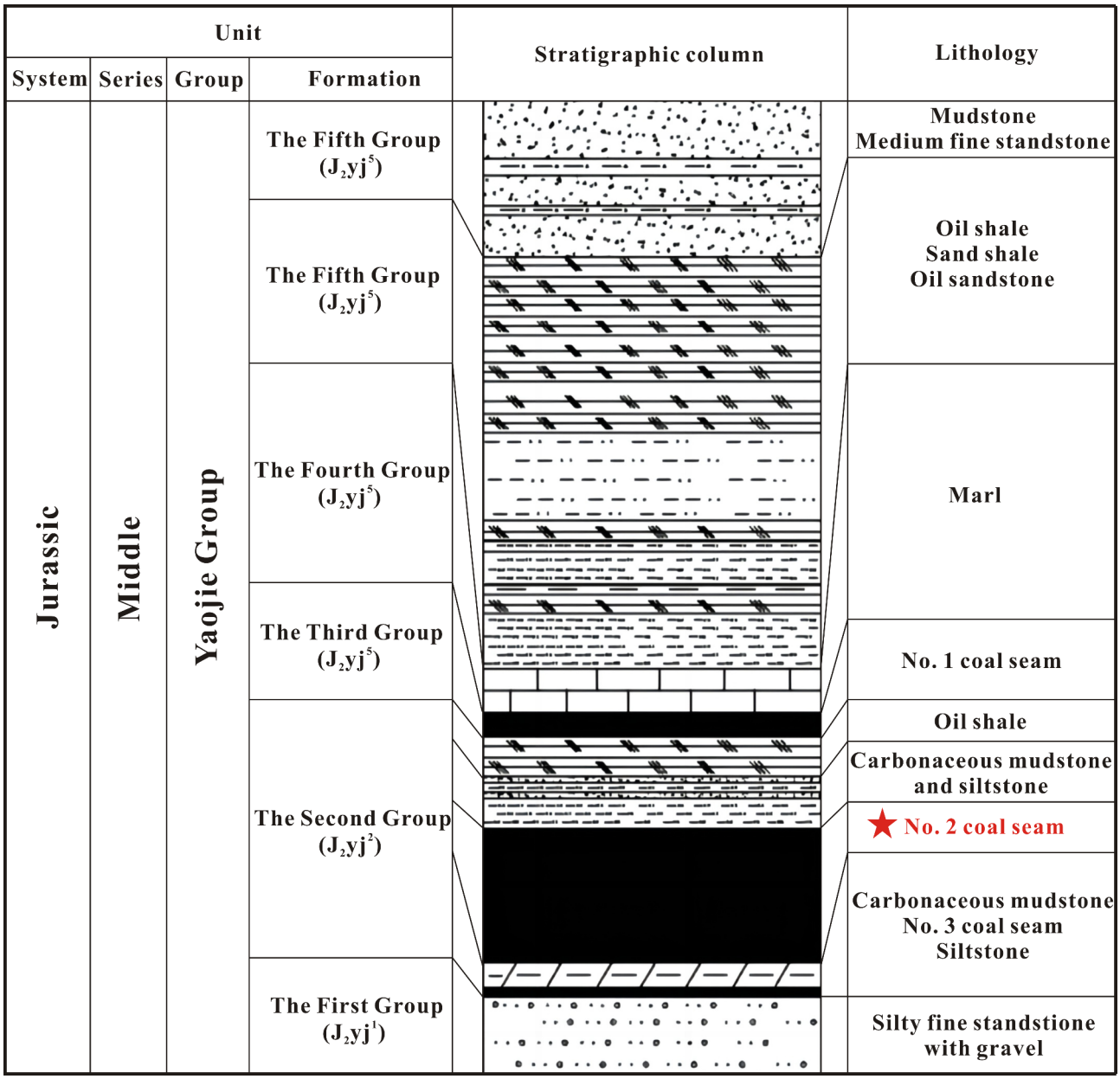

Fig. 2. Columnar section of coal-bearing strata in Haishiwan coal mine.

Adsorption heat measurement

In this study, C80 microcalorimeter was used to investigated the exothermic characteristics of the adsorption process. The C80 microcalorimeter was produced by Setaram Company, France, and consisted of a C80 host and a gas circulating pool. Coal sample was crushed and graded using standard sifters (0.18 mm to 0.15 mm), and dried for 24 h in a drying oven at 65℃ until the change between successice weights was < 0.001 g. The experimental temperature and pressure were set at 20 ℃, 30 ℃, 40 ℃, 50 ℃ and 1 MPa, 2 MPa, 3 MPa, 4 MPa, respectively. Meanwhile, CO_2 was selected as the adsorbed gas and the experimental time was set to 2 h.

Results and discussion

Gas component characteristics

CO_2 is the main gas component of CBG in the No.2 coal seam, among which the CO_2 concentration ranges from 15.47 to 90.67% (average 53.06%), and its content ranges from 1.1 m^3/t to 10.22 m^3/t. The CH_4 concentration in the No.2 coal seam varies from 2.02 to 80.04% (average 31.35%), and its content ranges from 0.17 m^3/t to 11.82 m^3/t. From Fig. 4a, No.2 coal seam has high contents of CBG in the east and central portion, contrasting with comparatively low contents in the west. The CO_2 content follows this pattern (Fig. 4b), while the CH_4 content shows different characteristics, with high levels in the south and west but lower levels in the north and east (Fig. 4c).

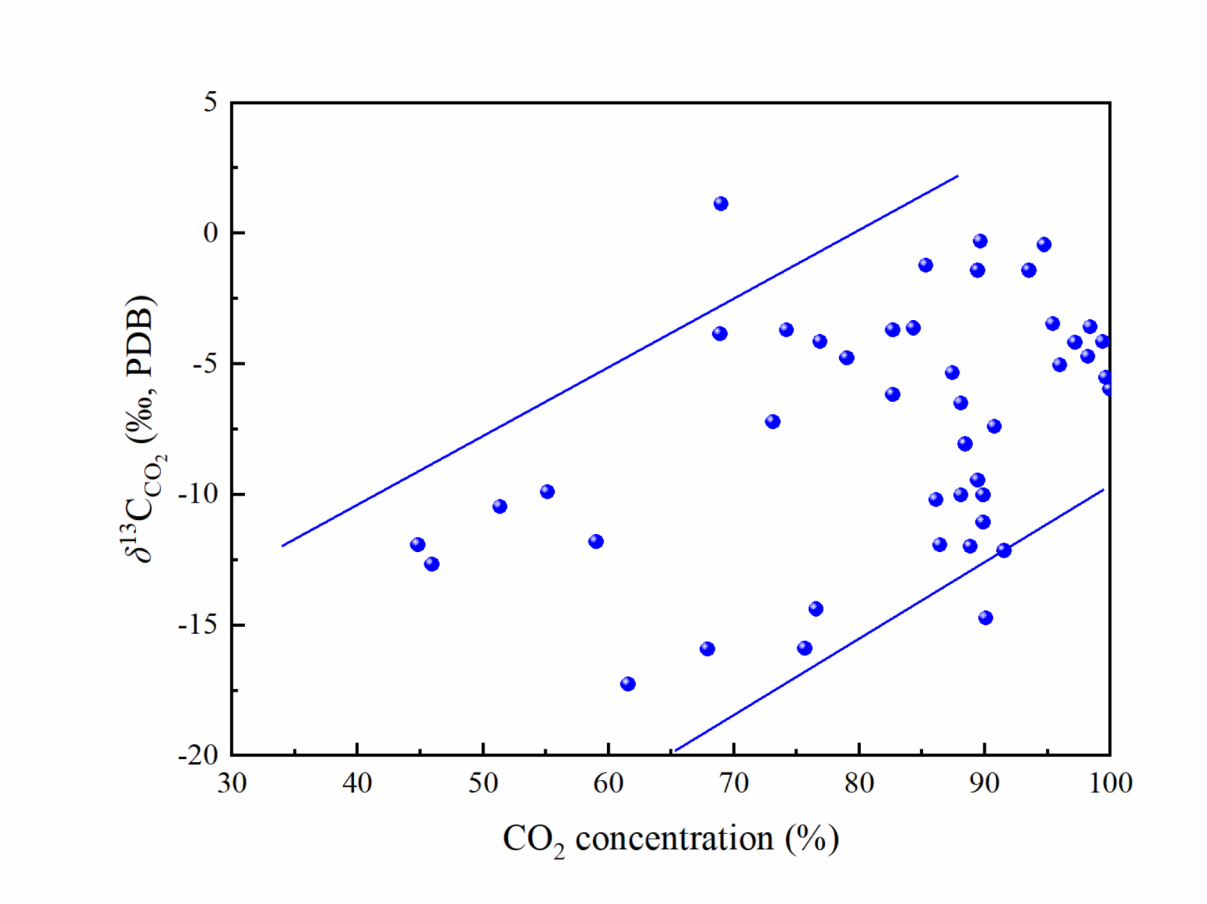

Fig. 3. CO_2 concentration and $\delta^{13}C_{CO2}$ (PDB) values for CO_2 from the No.2 coal seam in the Yaojie coalfield (data from Tao et al.[26] and Li et al.[27]).

Well no.	Buried depth (m)	Thickness (m)	Roof and floor lithology	Distance to F_{19} fault (m)	Completion horizon	Total drilling depth (m)	Completion method
D8#	1,092.5	31.6	The roof is argillaceous siltstone and the floor is sandy mudstone.	1,080	Proterozoic Metamorphic rock	1180	Casing completion
D5#	941.57	15.65	The roof is mudstone and the floor is sandy mudstone.	1,500		1048	
D6#	877.06	40.07	The roof is mudstone and the floor is fine sandstone.	820		945	
D2#	674.78	36.77	The roof is fine-grained sandstone and the floor is mudstone.	186	Middle Jurassic Yaojie group	725	

Table 1. Engineering overview of CBG wells.

Characteristics of CBG well drainage

The dynamic curves of gas and water production over time of four CBG wells are shown in Fig. 5. It can be seen that, (1) when the casing pressure was present in each well, the pressure of No.2 coal seam was 8 MPa to 9 MPa after adjusting for the bottom hole pressure. (2) The steady increase stage of gas production in each well is the uniformly decreasing stage of bottom hole flowing pressure, independent of casing pressure variations. (3) The water production of each well has a significant effect on its production capacity. The water production of the wells shows an evident downward trend after gas production. It is concluded that the production capacity of each well continues to decline after the steady pressure drainage. The reason for this is that the drainage intensity decreases and the water production decreases. Water turbulence is a mass transfer process, and the desorption of the coal seam requires the energy provided by water turbulence[32].

The gas production of wells D8#, D6#, and D2# declines after the production peak, while the gas production of well D5# continues to increase. According to the gas production characteristics of four CBG wells, the gas production types of CBG wells can be classified into three categories. (1) Rising. The gas production continues to increase over the drainage time, as seen in well D5#. (2) Multi-peak. Multiple peaks in gas production, such as those at wells D6# and D8#, are a regular occurrence. The maximum daily gas production of well D6# during

Parameters	Description/assumption
Grid system	Cartesian grid system with I × J × K = 30 × 30 × 1
Grid dimension	Each grid in x-direction = 10 m Each grid in y-direction = 10 m
Layers in the model	1
Fracture porosity, φ	From well-test data
Initial reservoir pressure, psi	From well-test data
Gas content, m^3/t	From gas content data
Gas composition	CH_4 and CO_2
Permeability, mD	From logging data
Perm anisotropy	PERMX = PERMY (no perm anisotropy)
Anisotropy permeability ratio	0.1
Initial water saturation, S_{wi}	100%
Reservoir temperature, ℃	Derived from depth

Table 2. Model description and assumptions.

drainage after 108 days is 1,210 m^3/d, decreasing to 900 m^3/d after 200 days. Then the gas production began to rise to 1,173 m^3/d after 228 days, decreasing to 825 m^3/d after 270 days. The production decline rate during the drainage time is 31.82%, and the average daily decline rate is 0.20%. The maximum daily gas production of well D8# during drainage after 179 days is 1,015 m^3/d, decreasing to 800 m^3/d after 244 days. The production decline rate during this period is 21.18%, and the average daily decline rate is 0.32%. The pump accidence happened around the 200st day of drainage, resulting in the occurrence of multiple peaks in the gas production curve. (3) Steady. The primary features of the gas production curve of this type, like well D2#, are a long constant production period and a reasonably stable gas production rate. The maximum daily gas production of well D2# during drainage after 117 days is 1,100.7 m^3/d, decreasing to 562.5 m^3/d after 535 days. The production decline rate during this period is 48.90%, and the average daily decline rate is 0.12%.

Well D2# took a longer drainage time with 535 days. Combined with the mechanism of CBG drainage, its drainage process can be classified into four stages. (I) Water production stage. During this stage with the maintenance time of 81 days, while the cumulative water production is 358.91 m^3, and the average water production is 4.49 m^3/d. (II) Rapid increase stage of gas production. This stage is characterized by a sharp increase in gas production and a decrease in water production, while the maximum gas production of 1,100.7 m^3/d was achieved after 117 days. (III) Stable stage of gas production. The gas production gradually declines from its peak and tends to stabilize, while the water production remains relatively stable at lower level. The cumulative gas production is 228,331.5 m^3, and the average gas production is 864.89 m^3/d. (IV) Decline stage of gas production. During this stage, gas production begins to decline slowly and will continue for an extended period of time.

Study on capacity simulation of CBG wells

Historical fitting of CBG wells

According to the CO_2 content of CBG wells based on Table 3, the gas production changes under different CO_2 concentrations of 20%, 50%, 60%, and 70% were simulated.

The key parameters for numerical simulation include buried depth, coalbed thickness, gas content of coalbeds, CH_4 content, CO_2 content, reservoir temperature, porosity, permeability, etc. The accuracy of parameter selection influences the numerical simulation results[33]. Based on the analysis of production data and referencing the geological parameters of four wells, the porosity, permeability, gas content, reservoir temperature, and other parameters were determined. After multiple parameter adjustments and fitting, the actual curve was visually compared with the fitted curve to determine the accuracy of the fitting results. The daily gas production fitting curves are shown in Fig. 6, and the parameters are detailed in Table 4.

Effect of various CO_2 concentrations on CBG production capacity

Based on the historical fitting parameters, the gas production of four wells in the next decade was simulated (Fig. 7), and the drainage data is shown in Table 5. The time from the start of drainage to continuous gas production is defined as the gas breakthrough time. The time from the start of gas breakthrough to the peak of gas production is defined as the peak production period. In the next decade, well D5# will continue to expand its gas production range, and the gas production rate will gradually decrease after reaching a peak of 3,150 m^3/d. Well D8# has the lowest gas production, with a maximum gas production of only 1,015 m^3/d. The gas production of four wells will decrease and gradually stabilize in the next decade, but the average gas production of wells D5# and D6# will remain above 800 m^3/d, with good gas production efficiency. The production decline rate of each well is different, among which well D5# has the largest production decline rate of 53.97%. In addition, the gas breakthrough time of CBG wells increases linearly with the increase of CO_2 concentration, in the order of 38→35→68→81 d.

Dewatering is a crucial stage for gas production in CBG reservoirs, and more dewatering means that the methane recovery factor would be lower[34]. As shown in Fig. 8, gas content changes synchronously with gas production, water production has a negative correlation between gas content and gas production. That is, CBG

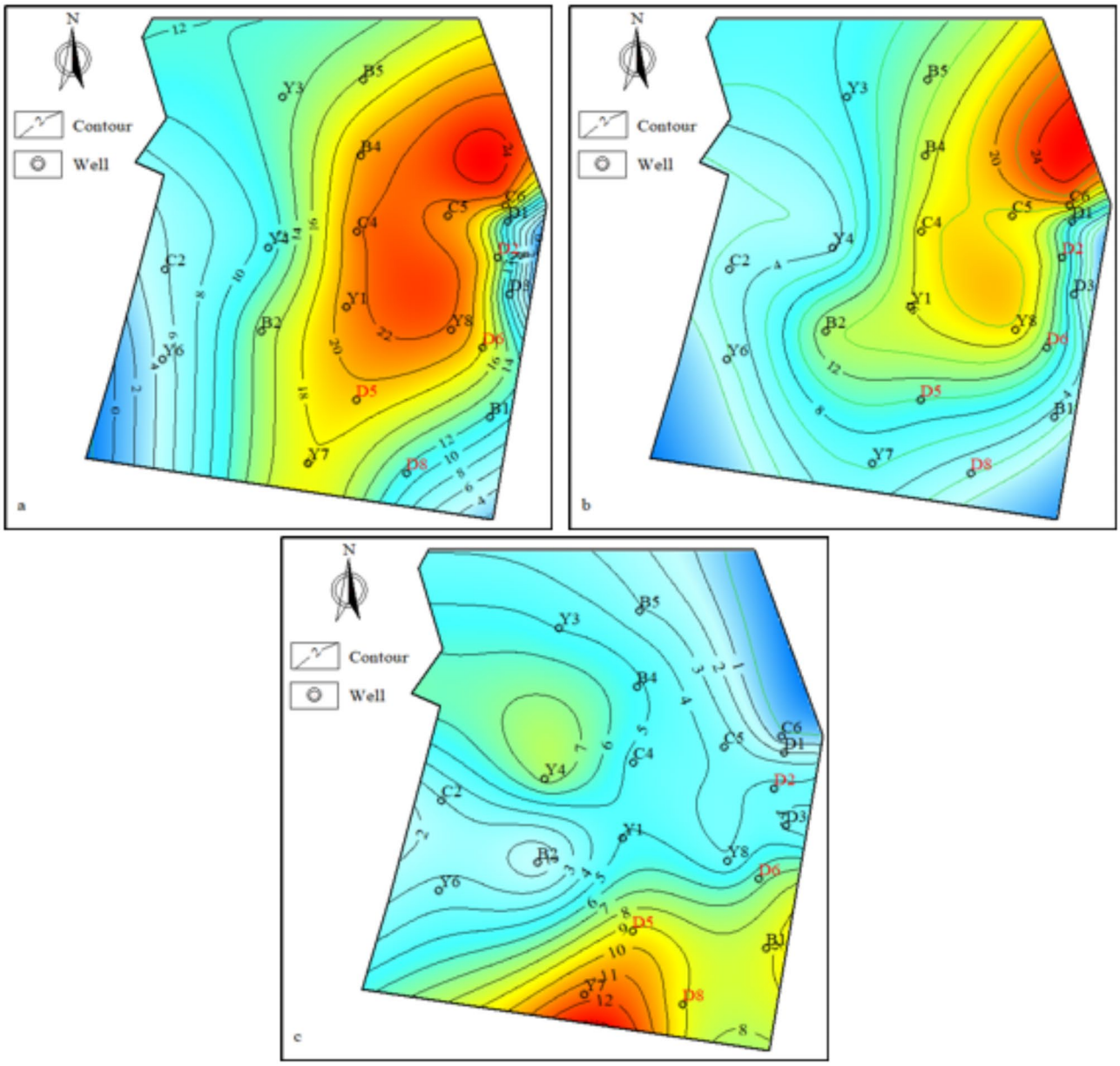

Fig. 4. Contour maps of gas distribution in the No.2 coal seam. (**a**) CBG, (**b**) CO_2 content, (**c**) CH_4 content (this figure is generated in DoubleFox V5.3.CO software, https://www.gdfoil.com/).

wells with higher water production have lower gas content and poorer gas production efficiency. This is consistent with the findings of Stevens et al.[35] and Asif et al.[34]. At the CO_2 concentration of 20%, the gas production and peak production period are low, while the water production is high. When the CO_2 concentration reaches 50%, the performance of CBG production increases, specifically with the maximum daily gas production increasing to 1,450.04 m^3/d and the peak production period increasing to 329 days. Meanwhile, the water production decreases. As the CO_2 concentration continues to increase, the gas production and peak production period decrease to the lowest point, while the water production increases (Fig. 9). This indicates that CBG wells with higher CO_2 concentration have lower gas production, higher water production, slower declines in gas production rate, and longer gas production period.

Compared with previous studies, there exists a critical mole fraction (~30%) in the binary gas adsorption process involving CO_2 and CH_4. Above this threshold, CO_2 becomes the predominant adsorbed phase on coal surfaces[22], leading to enhanced CH_4 desorption. This finding shares similarities with the results of our study. However, during the CO_2-ECBM process, the injection of CO_2 results in an increase in the CH_4 recovery rate. As the amount of injected CO_2 increases, the CH_4 production rate decreases, while the cumulative gas production initially rises and subsequently stabilizes[36,37]. This means that as the CO_2 concentration in the coal seam increases, so does the gas production. This differs from the results of this study. The reason for this discrepancy is that previous research has focused on reservoirs with high CH_4 content. Based on the competitive adsorption

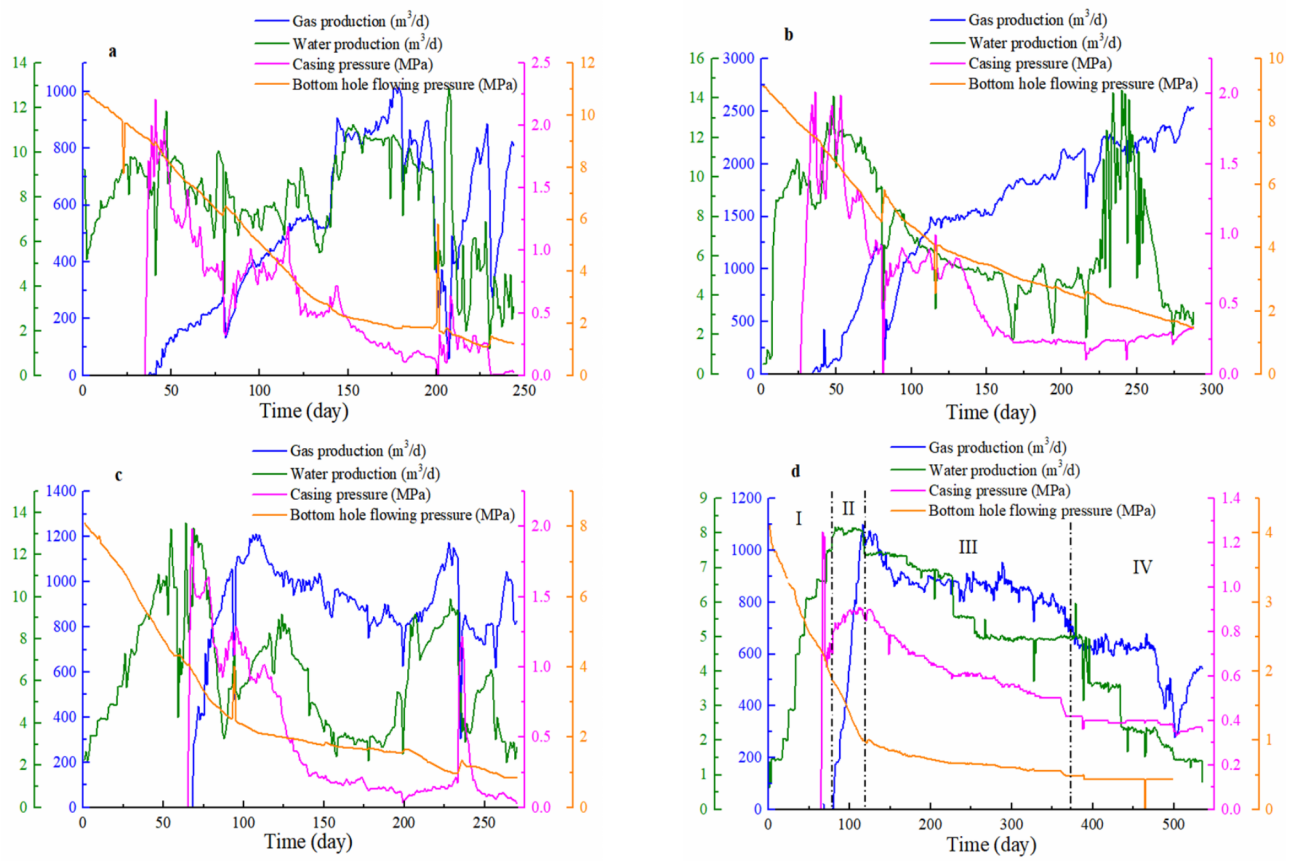

Fig. 5. Drainage curves of CBG wells. (**a**) well D8#, (**b**) well D5#, (**c**) well D6#, (**d**) well D2#.

Well no.	CH_4 content (m^3/t)	CO_2 content (m^3/t)	Gas content (m^3/t)	CO_2 concentration (%)
D8#	9.02	2.25	11.27	20
D5#	9.23	10.00	19.23	50
D6#	6.59	11.22	17.81	60
D2#	4.20	10.80	15.00	70

Table 3. Gas component content of CBG wells.

between CO_2 and CH_4, an increase in CO_2 injection results in a stronger displacement ability and a more thorough desorption of CH_4. In contrast, the research object in our study is a high CO_2 content reservoir, where the coal seam itself has a low CH_4 content. Consequently, the gas production after drainage and desorption is relatively low in that case.

Thermodynamic reasons affecting productivity differences of CBG wells

Geological reasons for changes in CBG production capacity

Previous studies have shown that buried depth and tectonics are key geological factors affecting the production capacity of CBG wells, mainly achieved through influencing gas adsorption. From Figs. 10 and 11, as the buried depth and distance to the F_{19} fault increase, CO_2 concentration decreases while CH_4 concentration increases. The reason is that the F_{19} fault is the main channel for CO_2 migration, and tectonic movements cause the rupture of coal seams near the F_{19} fault zone, increasing their porosity. Due to the significant adsorption capacity of coal seams for CO_2, they become the primary reservoir for CO_2 migration, leading to high CO_2 concentrations in the coal seams close to the F_{19} fault. Subsequently, CO_2 migrates from east to west in the coal seam, displacing CH_4 in the process. Tectonic movements have also caused the coal seams in the central and southern parts of the coalfield to be deeper, while those in the northern and eastern parts are relatively shallower (Fig. 12). Thus, with increasing distance to the F_{19} fault, buried depth increases, and CO_2 concentration decreases.

As shown in Fig. 13, the gas content and gas production of CBG wells change synchronously, both showing a trend of initially increasing and then decreasing with the increase of buried depth. This indicates a clear positive correlation between gas content and gas production. This is because the positive and negative effects of pressure and temperature on gas adsorption, which alter the gas content and consequently influence gas production.

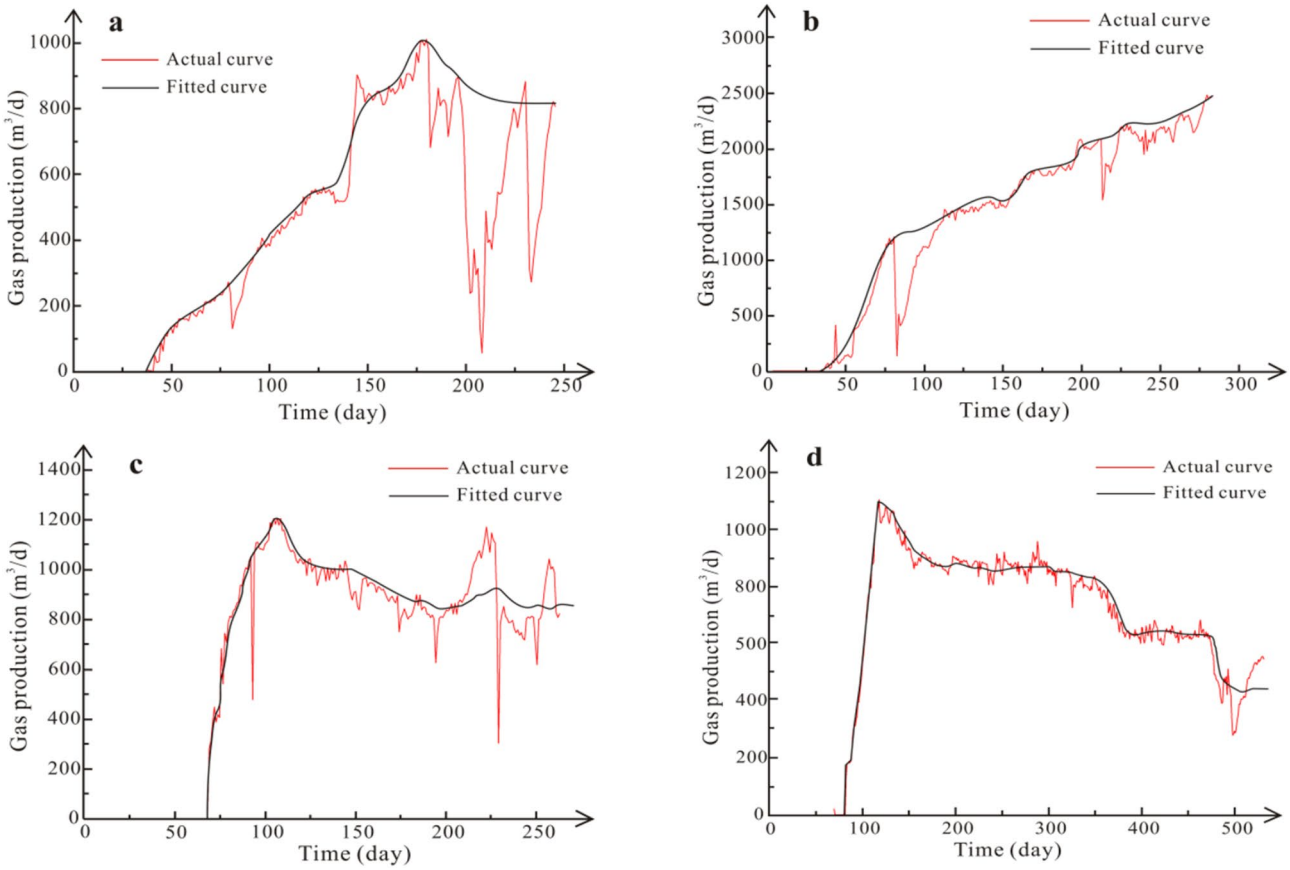

Fig. 6. Comparison of fitted and initial gas production curves. (**a**) well D8#, (**b**) well D5#, (**c**) well D6#, (**d**) well D2#.

Well no.	Parameters	Initial value	Fitted value	Parameters	Initial value	Fitted value
D2#	Buried depth (m)	674.78	674.78	CO_2 content (m^3/t)	10.80	10.80
	Coal seam thickness (m)	36.77	36.77	Reservoir temperature (℃)	33.99	33.99
	Gas content (m^3/t)	15.00	15.00	Porosity (%)	6.00	8.00
	CH_4 content (m^3/t)	4.20	4.20	Permeability (mD)	0.03	0.02
D5#	Buried depth (m)	941.57	—	CO_2 content (m^3/t)	10.0	—
	Coal seam thickness (m)	15.65	—	Reservoir temperature (℃)	42.1	—
	Gas content (m^3/t)	19.23	—	Porosity (%)	1.0	—
	CH_4 content (m^3/t)	9.23	—	Permeability (mD)	0.02	—
D6#	Buried depth (m)	877.06	—	CO_2 content (m^3/t)	11.22	—
	Coal seam thickness (m)	40.07	—	Reservoir temperature (℃)	40.14	—
	Gas content (m^3/t)	17.81	—	Porosity (%)	1.00	—
	CH_4 content (m^3/t)	6.59	—	Permeability (mD)	0.013	—
D8#	Buried depth (m)	1092.50	1092.5	CO_2 content (m^3/t)	2.25	2.25
	Coal seam thickness (m)	31.60	31.60	Reservoir temperature (℃)	46.69	46.69
	Gas content (m^3/t)	11.27	11.27	Porosity (%)	1.00	3.00
	CH_4 content (m^3/t)	9.02	9.02	Permeability (mD)	0.018	0.01

Table 4. Comparison of initial parameter values and historical fitting values.

According to Fig. 14, at buried depths shallower than 950 m, pressure plays a dominant role in promoting gas adsorption, leading to an increase in gas content. Conversely, at buried depths deeper than 950 m, temperature becomes the dominant factor, inhibiting gas adsorption and resulting in a decrease in gas content[2]. Coal seams provide a space for the adsorption of multiple gases. However, competitive adsorption occurs due to the different

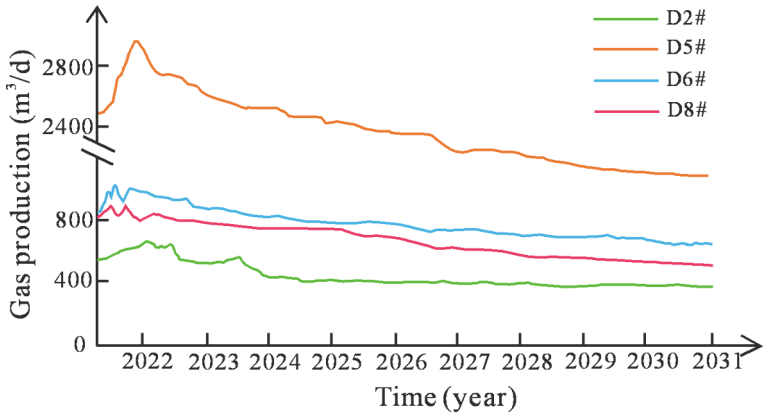

Fig. 7. Capacity prediction curves of CBG wells in the next decade.

Well no.	CO_2 concentration (%)	Gas content (m^3/t)	Maximum gas production (m^3/d)	Average gas production (m^3/d)	Gas breakthrough time (d)	Production decline rate (%)	Maximum water production (m^3/d)	Average water production (m^3/d)
D8#	20	11.27	1,015.0	517.00	38	49.06	12.88	6.85
D5#	50	19.23	3,150.0	1,450.04	35	53.97	14.42	3.88
D6#	60	17.81	1,210.0	800.00	68	43.80	13.51	4.24
D2#	70	15.00	1,100.7	562.50	81	48.89	8.18	4.73

Table 5. Drainage data of CBG wells.

affinities of CH_4 and CO_2 for coal, leading to variations in gas content and composition. This will be elaborated in "Thermodynamic mechanism of the impact of gas adsorption differences on productioncapacity" section.

Thermodynamic mechanism of the impact of gas adsorption differences on production capacity

To explore the thermodynamic mechanism affecting production capacity differences, experiments were conducted on the adsorption heat of CO_2 and CH_4 on coal with medium metamorphic degree under different temperature and pressure conditions, as shown in Figs. 15, 16 and 17. The adsorption heat of CO_2 and CH_4 increases with the increase of pressure and the decrease of temperature. And under constant pressure, the variation in CH_4 adsorption heat across different temperatures is relatively minor, whereas the difference in CO_2 adsorption heat is significant. This suggests that temperature has a lesser impact on CH_4 adsorption heat compared to CO_2, which is more sensitive to temperature changes. On one hand, as the temperature increases, the movement of gas molecules intensifies and then gas molecules are less likely to be adsorbed on coal, leading to the adsorption heat of CO_2 and CH_4 decrease. On the other hand, increased pressure results in a decline in the distance between the coal surface and gas molecules, which increases Van der Waals forces and promotes collision frequency between the coal surface and gas molecules, thereby promoting coal adsorption onto the gas[39,40]. This results in an increase in the adsorption heat of CO_2 and CH_4. That is, in high-temperature and high-pressure environments, CO_2 cannot be adsorbed in significant quantities and remains in a free state, thereby providing more opportunities for CH_4 to be adsorbed.

Notably, the heat released during the adsorption of CO_2 is greater than that released during the adsorption of CH_4 (Fig. 16), suggesting that CO_2 has a stronger adsorption capacity than CH_4. Li[42] and Wang[43] conducted isothermal adsorption experiments of CO_2/CH_4 mixed gas on coal samples from Haishiwan coal mine, confirming that CO_2 has a stronger adsorption capacity than CH_4. Moreover, as the CO_2 concentration in the mixed gas increases, the total adsorption capacity of coal on the mixed gas also increases (Fig. 18). Because of the quadrupole moment structure of CO_2 molecules, which is highly sensitive to polarity, the presence of polar oxygen-containing functional groups in coal creates additional adsorption sites for CO_2, thereby enhancing its adsorption on the coal surface[44]. In contrast, CH_4 molecules, being non-polar, exhibit a weaker interaction with the coal surface and consequently possess a reduced adsorption capacity. Meanwhile, the kinetic diameter of CO_2 (0.33 nm) is smaller than that of CH_4 (0.38 nm), making it easier to diffuse into micropores, resulting in an increase in CO_2 adsorption[45]. Therefore, the higher the CO_2 concentration in the coal seam, the greater the gas content. Combined with "Geological reasons for changes in CBG production capacity" section, it can be seen that near the F_{19} fault, the coal seam is shallow, exhibiting a high CO_2 concentration and a correspondingly high gas content.

CBG drainage is a dynamic process of adsorption and desorption. During the drainage process, CH_4 continuously desorbs, adding adsorption sites for CO_2, resulting in an increase in CO_2 concentration. The higher the CO_2 content, the greater the pressure reduction required to achieve the same desorption amount, which is

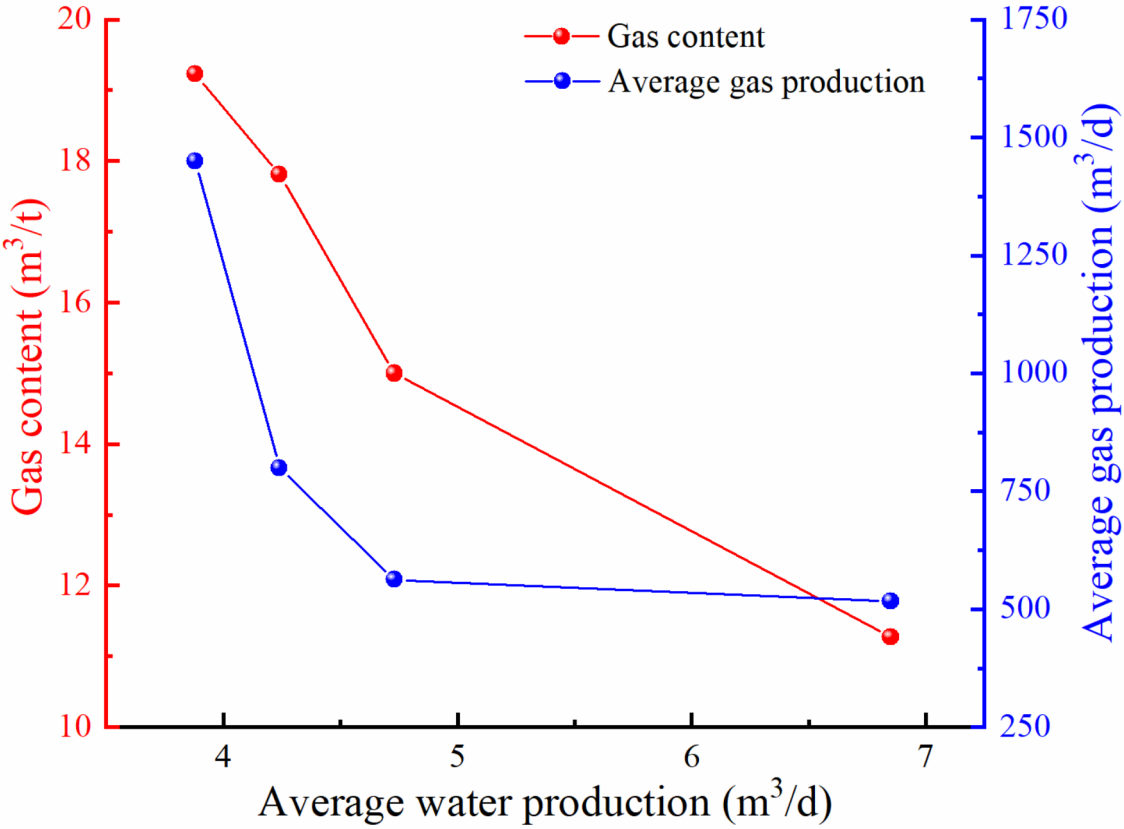

Fig. 8. Relationship between water production, gas content, and gas production.

not conducive to gas desorption and makes CBG drainage more difficult. Therefore, CBG wells with high CH_4 concentration usually have earlier gas breakthrough time and higher gas content. Correspondingly, CBG wells with high CO_2 concentration have slower ga breakthrough and lower gas production. However, it is should be noted that gas produced from CBG wells is a mixture of free gas and adsorbed gas. The gas production is not solely determined by the content of adsorbed gas, but this underscores the complexity and variability of coal adsorption mechanisms and their role in CBG drainage. Therefore, it highlights the need for further research to deepen our understanding of the exploitation mechanisms of CO_2-rich CBG wells.

Conclusions

(1) The production types of CBG wells are classified into rising, multi-peak, and stable types based on gas production characteristics. The rising type shows continuous gas production growth with a good gas production performance, while the multi-peak type fluctuates significantly. The stable type has a longer gas production period with stable gas production.
(2) Simulation results indicate that CO_2 concentration limits the CBG production capacity. A higher CO_2 concentration in a CBG well is associated with a later gas breakthrough time, increased water production, a longer gas production period, and poorer CBG production capacity.
(3) CBG production capacity is affected by geological factors, mainly through the influencing of temperature and pressure on gas adsorption. High pressure increases gas content by promoting adsorption, thereby boosting production. However, CO_2's stronger adsorption compared to CH_4 raises CO_2 concentrations, hindering desorption, causing slower gas breakthrough, and a longer production period. Conversely, high temperature inhibits adsorption, lowering CO_2 concentration and gas content, which promotes CH_4 desorption, accelerates gas breakthrough, ultimately reduces production.

The findings from this comprehensive experiments and numerical simulation provide valuable guidance for future CBG development in CO_2-rich coalfields, similar to the Yaojie coalfield. However, further studies of the

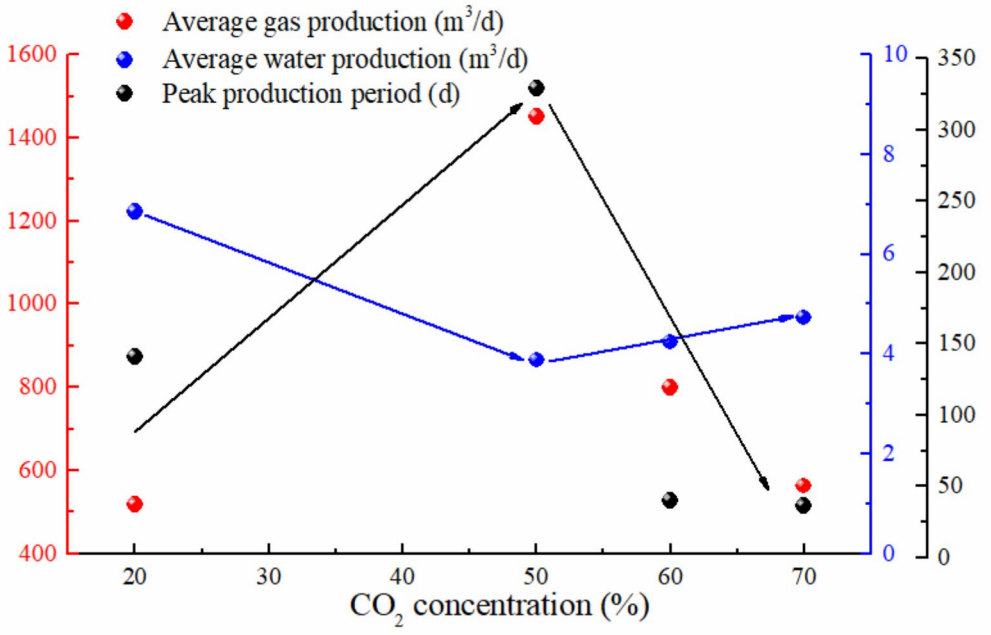

Fig. 9. The trend of changes in gas production, water production, and peak production period with CO_2 concentration.

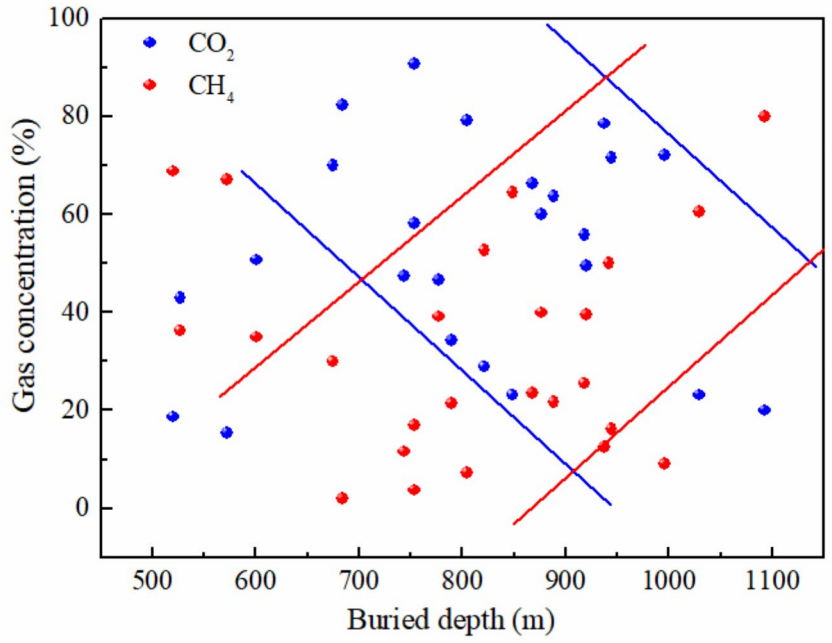

Fig. 10. Relationship between buried depth and CO_2/CH_4 concentration.

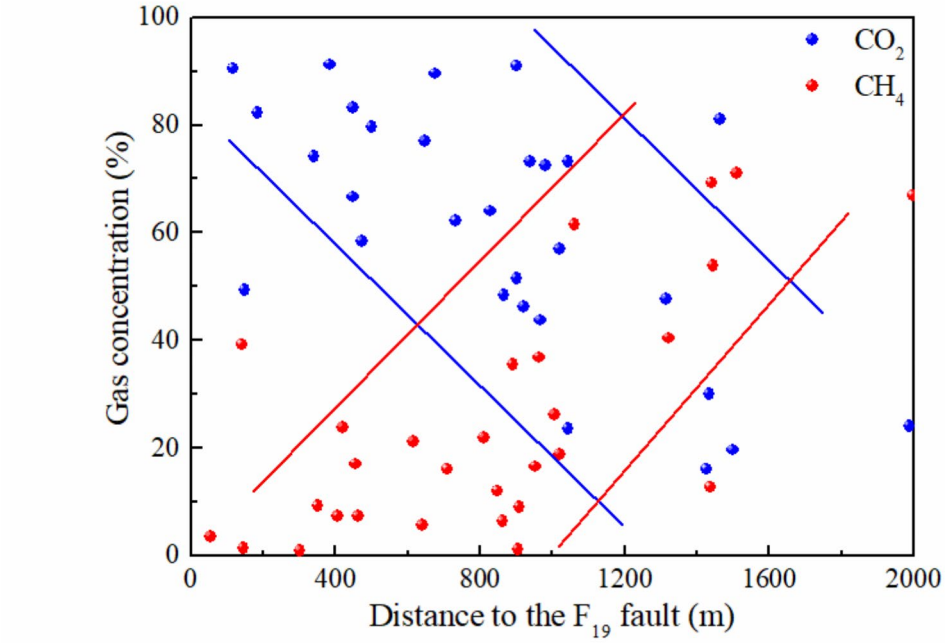

Fig. 11. Relationship between distance to the F_{19} fault and CO_2/CH_4 concentration.

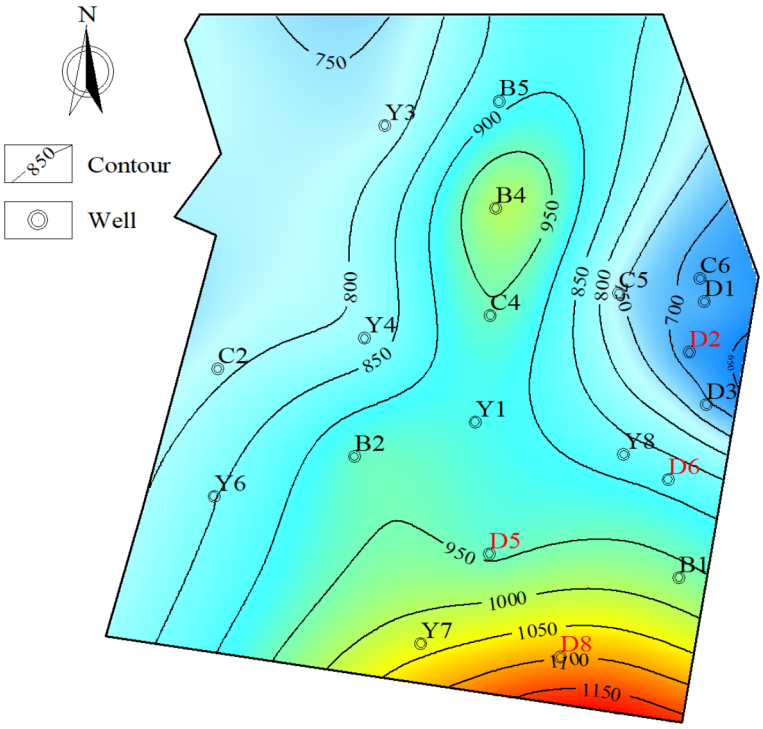

Fig. 12. Contour map of buried depth of No.2 coal seam (this figure is generated in DoubleFox V5.3.CO software, https://www.gdfoil.com/).

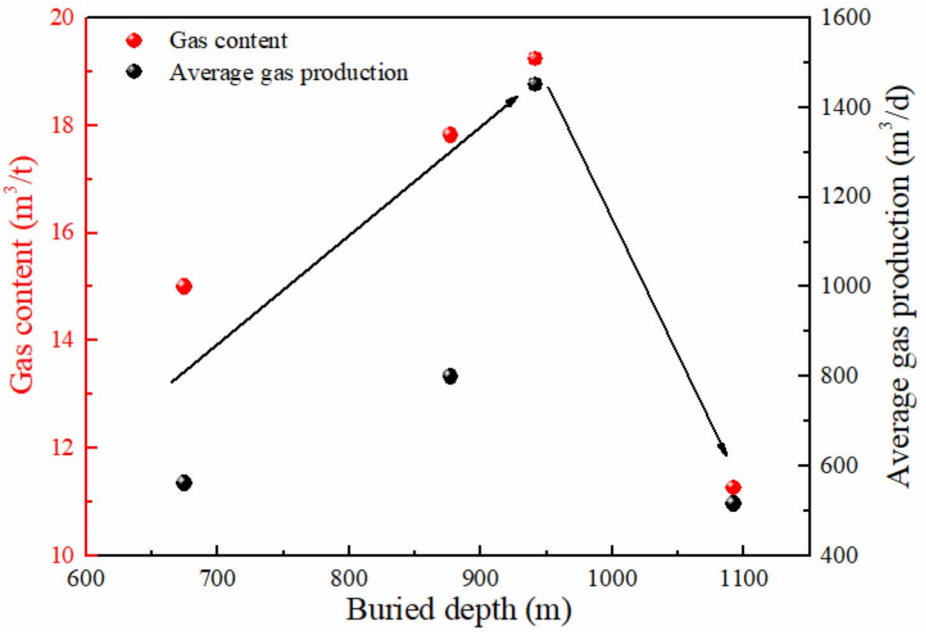

Fig. 13. Relationship between buried depth, gas content, and gas production of CBG wells.

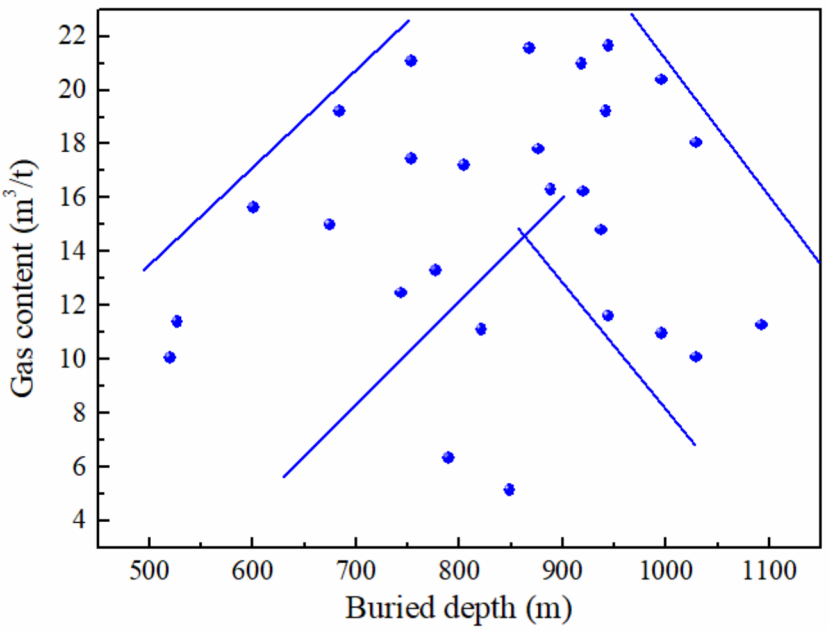

Fig. 14. Relationship between buried depth and gas content in Haishiwan coal mine.

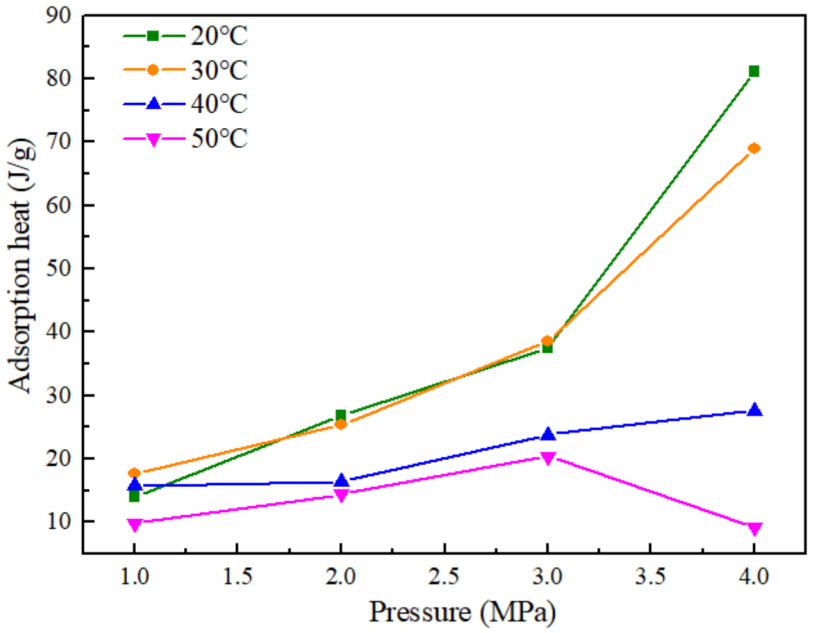

Fig. 15. CO_2 adsorption heat characteristics of the coal.

.

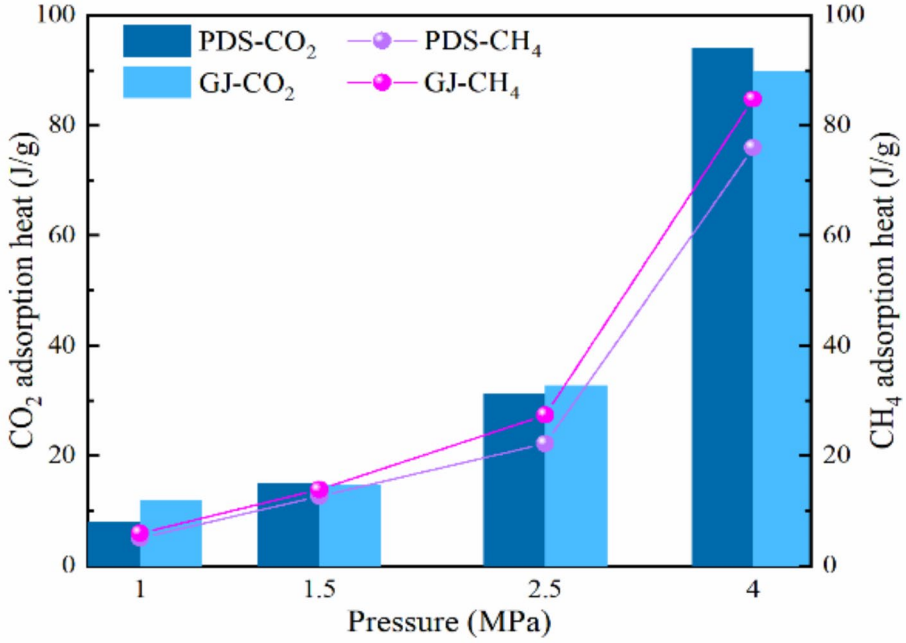

Fig. 16. Adsorption heat of CO_2 and CH_4 at different pressure (at 30 ℃) (data from Zhang et al.[38]).

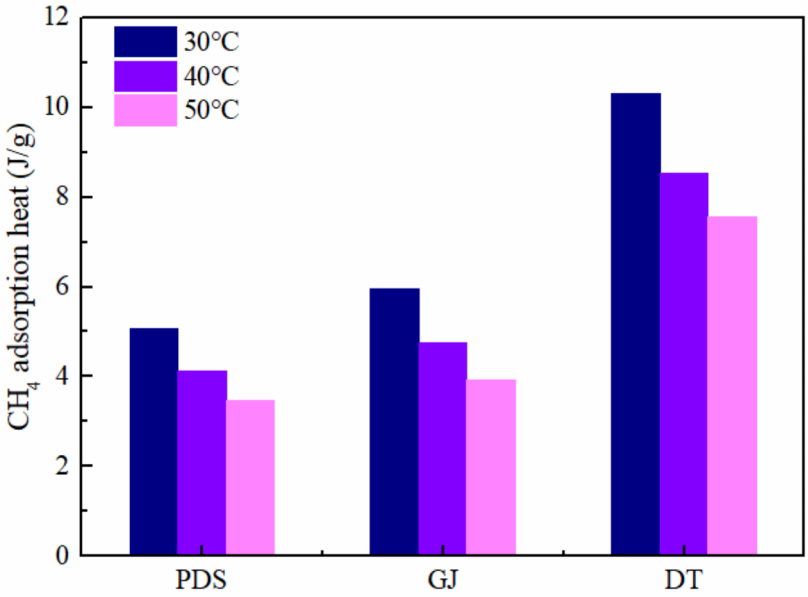

Fig. 17. Adsorption heat of CH_4 at different temperatures (at 1 MPa) (data from Zhang et al.[38], and Li et al.[41]).

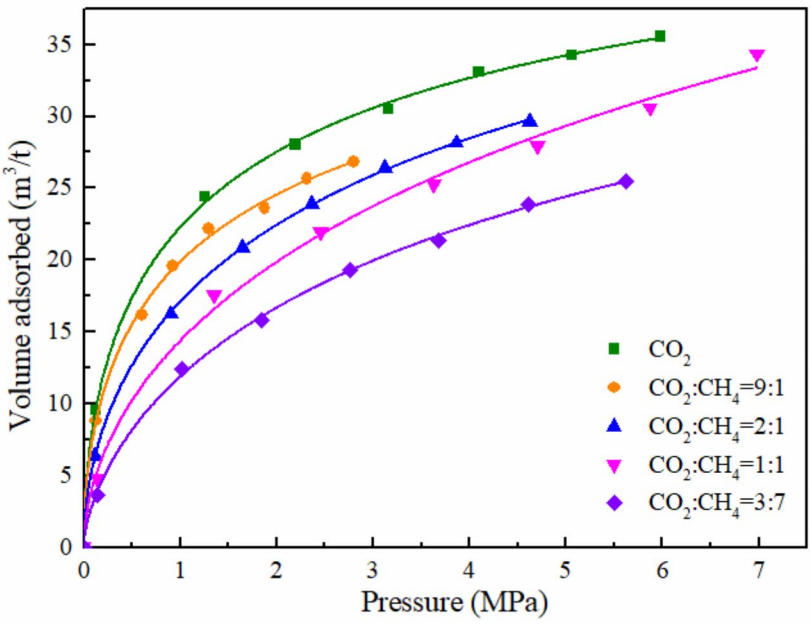

Fig. 18. Adsorption isotherm of CO_2/CH_4 mixed gas (at 30 ℃) (data from Li[42]).

impact of reservoir properties on the coal adsorption mechanism is crucial for advancing our understanding of the development mechanisms of CO_2-rich CBG wells.

Data availability

Data is provided within the manuscript.

Received: 17 May 2024; Accepted: 5 March 2025
Published online: 18 March 2025

References

1. Bamberger, I., Stieger, J., Buchmann, N. & Eugster, W. Spatial variability of methane: Attributing atmospheric concentrations to emissions. *Environ. Pollut.* **190**, 65–74 (2014).
2. Tao, S., Shang, D., Hu, H., Lv, Y. & Zhao, X. Analysis on influence factors of CBM wells productivity and development proposals in Southern Qinshui basin. *J. China Coal Soci.* **36**(2), 194–198 (2018).
3. Feng, R. Y. A method to evaluated gas content with coalbed methane reservoir based on adsorption theory and production analysis. *Geofluids* **7341886** (2022).
4. Liu, B. et al. Coalbed methane gas content and its geological controls: Research based on seismic-geological integrated method. *J. Nat. Gas Sci. Eng.* **101**, 104510 (2022).
5. Tang, S. et al. Controlling factors of CBM well productivity of multiple superposed CBM systems: A case study on the Songhe well-field, Guizhou, China. *Energy Explor. Exploit.* **35**(6), 665–684 (2017).
6. Wang, H. et al. Drainage type classification and key controlling factors of productivity for CBM wells in the Zheng Zhuang area, Southern Qinshui basin, North China. *ACS Omega*. **7**, 1883–1892 (2022).
7. Zhu, C. J. et al. Methane adsorption on coals with different coal rank under elevated temperature and pressure. *Fuel* **254**, 115686 (2019).
8. Lu, D. T. et al. Shale productivity prediction and fracturing optimization based on compositional simulation. *Chin. Sci. Bull.* **61**(1), 94–101 (2016).
9. Zhang, X. D., Zhao, J. P. & Zhang, S. Study on main control factors of gas drainage in coalbed methane well of Tunliu minefield. *Coal Sci. Technol.* **42**(6), 71–75 (2014).
10. Zhang, X. D., Zhang, S., Sun, Q. Y., Yang, Y. H. & Yang, Y. L. Evaluating the influence of geological structure to CBM productivity based on AHP and fuzzy mathematics. *J. China Coal Soc.* **42**(9), 2385–2392 (2017).
11. Vikram, V., Mahanta, B., Pradhan, S. P., Singh, T. N. & Ranjith, P. G. Simulation of CO_2 enhanced coalbed methane recovery in Jharia coalfields, India. *Energy* **159**, 1185–1194 (2018).
12. Mu, Y. L., Fan, Y. P., Wang, J. R. & Fan, N. Numerical study on the injection of heated CO_2 to enhance CH4 recovery in water-bearing coal reservoirs. *Energy Sources Part. A* (2019).
13. Hou, Y. D. et al. Numerical simulation of the effect of injected CO_2 temperature and pressure on CO_2-enhanced coalbed methane. *Appl. Sci.* **10**(4), 1385 (2020).
14. Zhou, F. D. History matching and production prediction of a horizontal coalbed methane well. *J. Pet. Sci. Eng.* **96–97**, 22–36 (2012).
15. Hu, Q. J. et al. Numerical analysis of drainage rate for multilayer drainage coalbed methane well group in Southern Qinshui basin. *Energy Explor. Exploit.* **38**(9), 1535–1558 (2020).
16. Huang, T., Liao, X., Huang, Z. Q., Song, F. Q. & Wang, R. Y. Numerical simulation of well type optimization in tridimensional development of multi-layer shale gas reservoir. *Energies* **15**(18), 6529 (2022).
17. Zhang, S. W., Zhang, M. Z., Wang, Z. & Yin, R. W. Research on shale gas capacity prediction method based on optimization algorithm. *J. Comb. Optim.* **45**(5), 123 (2023).
18. Cui, X. J., Bustin, R. M. & Dipple, G. Selective transport of CO_2, CH_4, and N_2 in coals: insights from modeling of experimental gas adsorption data. *Fuel* **83**(3), 293–303 (2004).
19. Busch, A., Krooss, B. M., Gensterblum, Y., Van Bergen, F. & Pagnier, H. J. M. High-pressure adsorption of methane carbon dioxide and their mixtures on coals with a special focus on the preferential sorption behaviour. *J. Geochem. Explor.* **7**(78), 671–674 (2003).
20. Harpalani, S., Prusty, B. K. & Dutta, P. Methane/CO_2 sorption modeling for coalbed methane production and CO_2 sequestration. *Energy Fuels* **20**(4), 1591–1599 (2006).
21. Zhou, L., Feng, Q. & Qin, Y. Thermodynamic analysis of competitive adsorption of CO_2 and CH_4 on coal matrix. *J. China Coal Soc.* **36**(8), 1307–1311 (2011).
22. Asif, M. et al. Influence of competitive adsorption, diffusion, and dispersion of CH_4 and CO_2 gases during the CO_2-ECBM process. *Fuel* **358**, 130065 (2024).
23. Zhang, L., Ren, T., Aziz, N. & Zhang, C. Evaluation of coal seam gas drainability for outburst-prone and high-CO_2-containing coal seam. *Geofluids* **3481834** (2019).
24. Black, D. J. Review of coal and gas outburst in Australian underground coal mines. *Int. J. Min. Sci. Technol.* **29**, 815–824 (2019).
25. Tao, M. X., Chen, F. Y. & Xu, Y. C. The evolution and structural characteristics of Yaojie F_{19} fracture zone. *Coal Geol. China*. **7**, 12–16 (1995).
26. Tao, M. X., Xu, Y. C., Chen, F. Y., Shen, P. & Sun, M. L. Helium isotope characteristics and significance of carbon dioxide gas in Yaojie coalfiled. *Chin. Sci. Bull.* **12**, 921–923 (1991).
27. Li, W., Cheng, Y. P. & Wang, L. The origin and formation of CO_2 gas pools in the coal seam of the Yaojie coalfield in China. *Int. J. Coal Geol.* **85**(2), 227–236 (2011).
28. Dai, J. X., Yang, S. F., Chen, H. L. & Shen, X. H. Geochemistry and occurrence of inorganic gas accumulations in Chinese sedimentary basins. *Org. Geochem.* **36**(12), 1667–1688 (2005).
29. Diamond, W. P. & Schatzel, S. J. Measuring the gas content of coal: A review. *Int. J. Coal Geol.* **35**, 311–331 (1998).
30. Asif, M., Panigrahi, D. C., Naveen, P. & Ojha, K. Construction of high-pressure adsorption isotherm: A tool for predicting coalbed methane recovery from Jharia coalfield, India. *Int. J. Min. Sci. Technol.* **29**, 765–769 (2018).
31. Sujoy, C., Rajeev, U., Debadutta, M., Gopinath, H. & Tarkeshwar, K. Evaluating production behaviour of CBM wells from Raniganj coalfield through reservoir characterization under constrained field data conditions. *J. Nat. Gas Sci. Eng.* **92**, 103969 (2021).
32. Ma, D. M. et al. CBM well drainage data-based dynamic inversion study of reservoir gas content. *Coal Geol. Explor.* **49** (6), 67–73 (2021).
33. Yao, P. et al. Effect of water occurrence in coal reservoirs on the production capacity of coalbed methane by using NMR simulation technology and production capacity simulation. *Geoenergy Sci. Eng.* **243**, 213353 (2024).
34. Asif, M., Wang, L., Panigrahi, D. C., Ojha, K. & Hazlett, R. Integrated assessment of CO_2-ECBM potential in Jharia coalfield, India. *Sci. Rep.* **12**, 7533 (2022).
35. Stevens, S. H., Spector, D. & Riemer, P. Enhanced coalbed methane recovery using CO_2 injection: Worldwide resource and CO_2 sequestration potential. *SPE International Oil and Gas Conference and Exhibition in China*, SPE-48881-MS (1998).
36. Tiyntayev, Y. et al. Simulation-based evaluation of concurrent CH_4 storage potentials during CO_2-ECBM in Karaganda coal basin. *SPE Annual Caspian Technical Conference* SPE212076-MS (2022).

37. Serikov, G., Wang, L., Asif, M. & Hazlett, R. Simulation evaluation of CO_2-ECBM potential in Karaganda coal basin in Kazakhstan. *SPE EuropEC - Europe Energy Conference featured at the 83rd EAGE Annual Conference & Exhibition* SPE-209698-MS (2022).
38. Zhang, S. et al. Molecular simulation of CH_4 and CO_2 adsorption behavior in coal physicochemical structure model and its control mechanism. *Energy* **285**, 129474 (2023).
39. Zhong, L. W. Adsorptive capacity of coals and its affecting factors. *J. China Univ. Geosci.* **29**(3), 327–332 (2004).
40. Li, L., Si, J. H., Li, Z. X., Cheng, G. Y. & Chen, J. C. Experimental study on influencing factors and thermal effects of CO_2 adsorption by coal. *ACS Omega.* **8**(24), 21906–21913 (2023).
41. Li, L. J., Zhang, L., Guo, J. Y., Liu, S. Y. & Zhang, S. H. Study on adsorption thermodynamics of CO_2 and CH_4 on coal by means of combination of high pressure gas adsorption and desorption-microcalorimeter. *Coal Convers.* **43**(3), 1–7 (2020).
42. Li, W. Mechanism of CO_2 pools formation and CO_2 control technology of Haishiwan coalfield. *China Univ. Min. Technol.* (2011).
43. Wang, L. G., Cheng, Y. P., Li, W., Lu, S. Q. & Xu, C. Component fractionation of temporal evolution in adsorption-desorption for binary gas mixtures on coals from Haishiwan coal mine. *Int. J. Min. Sci. Technol.* **2**, 201–205 (2013).
44. Huang, X. et al. Investigation of oxygen-containing group promotion effect on CO_2-coal interaction by density functional theory. *Appl. Surf. Sci.* **299**(2), 162–169 (2014).
45. Pajdak, A., Kudasik, M., Skoczylas, N., Wierzbicki, M. & Braga, L. T. P. Studies on the competitive sorption of CO_2 and CH_4 on hard coal. *Int. J. Greenh. Gas Control* **90**, 102789 (2019).

Acknowledgements

This work was supported by the National Natural Science Foundation of China, China (No. 42172198 and 42202210), Key Scientific Research Projects of Colleges and Universities in Henan Province (No. 23A44007), and Scientific and Technological Research Project in Henan Province, China (No. 232102320336).

Author contributions

Z.S. conducted the numerical simulation, analyzed the data and wrote the manuscript. X.Z. and S.Z. led the research and edited the manuscript. S.L. and J.Z.provided the research materials. C.W. and X.L. provided the theoretical background. All authors reviewed the manuscript.

Declarations

Competing interests

The authors declare no competing interests.

Additional information

Correspondence and requests for materials should be addressed to X.Z. or S.Z.

Reprints and permissions information is available at www.nature.com/reprints.

Publisher's note Springer Nature remains neutral with regard to jurisdictional claims in published maps and institutional affiliations.

Open Access This article is licensed under a Creative Commons Attribution-NonCommercial-NoDerivatives 4.0 International License, which permits any non-commercial use, sharing, distribution and reproduction in any medium or format, as long as you give appropriate credit to the original author(s) and the source, provide a link to the Creative Commons licence, and indicate if you modified the licensed material. You do not have permission under this licence to share adapted material derived from this article or parts of it. The images or other third party material in this article are included in the article's Creative Commons licence, unless indicated otherwise in a credit line to the material. If material is not included in the article's Creative Commons licence and your intended use is not permitted by statutory regulation or exceeds the permitted use, you will need to obtain permission directly from the copyright holder. To view a copy of this licence, visit http://creativecommons.org/licenses/by-nc-nd/4.0/.

© The Author(s) 2025